HHS Public Access

Author manuscript

Oncogene. Author manuscript; available in PMC 2020 January 19.

Published in final edited form as:

Oncogene. 2019 September ; 38(37): 6399–6413. doi:10.1038/s41388-019-0887-2.

Targeting FGFR overcomes EMT-mediated resistance in EGFR mutant non-small cell lung cancer

Sana Raoof[1,†], **Iain J. Mulford**[2,†], **Heidie Frisco-Cabanos**[1], **Varuna Nangia**[1], **Daria Timonina**[1], **Emma Labrot**[2], **Nafeeza Hafeez**[2], **Samantha J. Bilton**[1], **Yotam Drier**[1], **Fei Ji**[1], **Max Greenberg**[1], **August Williams**[1], **Krystina Kattermann**[1], **Leah Damon**[1], **Sosathya Sovath**[2], **Daniel P. Rakiec**[2], **Joshua M. Korn**[2], **David A. Ruddy**[2], **Cyril H. Benes**[1,3], **Peter S. Hammerman**[2], **Zofia Piotrowska**[1,3], **Lecia V. Sequist**[1,3], **Matthew J. Niederst**[2], **Jordi Barretina**[2], **Jeffrey A. Engelman**[2], **Aaron N. Hata**[1,3]

[1]Massachusetts General Hospital (MGH) Cancer Center, Charlestown, Massachusetts, USA.

[2]Oncology Disease Area, Novartis Institutes for Biomedical Research, Cambridge, Massachusetts, USA.

[3]Department of Medicine, Harvard Medical School, Boston, Massachusetts, USA.

Abstract

Evolved resistance to tyrosine kinase inhibitor (TKI) targeted therapies remains a major clinical challenge. In *EGFR* mutant non-small cell lung cancer (NSCLC), failure of EGFR TKIs can result from both genetic and epigenetic mechanisms of acquired drug resistance. Widespread reports of histologic and gene expression changes consistent with an epithelial-to-mesenchymal transition (EMT) have been associated with initially surviving drug tolerant persister cells, which can seed *bona fide* genetic mechanisms of resistance to EGFR TKIs. While therapeutic approaches targeting fully resistant cells, such as those harboring an $EGFR^{T790M}$ mutation, have been developed, a clinical strategy for preventing the emergence of persister cells remains elusive. Using mesenchymal cell lines derived from biopsies of patients who progressed on EGFR TKI as surrogates for persister populations, we performed whole-genome CRISPR screening and identified FGFR1 as the top target promoting survival of mesenchymal EGFR mutant cancers. Although numerous previous reports of FGFR signaling contributing to EGFR TKI resistance in vitro exist, the data has not yet been sufficiently compelling to instigate a clinical trial testing this hypothesis, nor has the role of FGFR in promoting the survival of persister cells been elucidated. In this study, we find that combining EGFR and FGFR inhibitors inhibited the survival and expansion of *EGFR* mutant drug tolerant cells over long time periods, preventing the development

Address correspondence to: Aaron N. Hata, Massachusetts General Hospital Cancer Center, 149 13th St, Boston, Massachusetts 02129, USA., ahata@mgh.harvard.edu.

[†]Equal contribution

Lead Contact: Aaron N. Hata

Author Contributions

S.R., I.J.M., M.J.N., J.A.E., and A.N.H. designed the study, analyzed the data and wrote the paper. S.R., I.J.M., H.F.C., V.N., E.L., N.H., L.D., J.M.K., S.S. and J.B. performed cell line and biochemical studies. S.R., D.T., and S.J.B. performed tumor xenograft studies. L.V.S. and Z.P. provided EGFR mutant patient samples. M.G., A.W., and K.K., generated patient-derived cell lines. D.A.R., Y.D., and F.J. performed computational analysis. All authors discussed the results and commented on the manuscript

of fully resistant cancers in multiple vitro models and in vivo. These results suggest that dual EGFR and FGFR blockade may be a promising clinical strategy for both preventing and overcoming EMT-associated acquired drug resistance and provide motivation for clinical study of combined EGFR and FGFR inhibition in EGFR-mutated NSCLCs.

Introduction

Non-small cell lung cancers (NSCLCs) that harbor activating EGFR mutations are sensitive to small molecule EGFR inhibitors, with responses observed in 60–70% of patients (1–4). Unfortunately, drug resistance inevitably develops, leading to disease progression. A number of mechanisms of irreversible, acquired resistance have been identified, including the $EGFR^{T790M}$ gatekeeper mutation, amplification of the MET receptor tyrosine kinase gene, histological transformation to small cell lung cancer (5–8), and FGFR signaling (9–13). Third generation EGFR inhibitors have now been developed that are capable of overcoming $EGFR^{T790M}$ (14, 15) and combination strategies that target MET-amplified resistant cancers are being evaluated in clinical trials, but no clinical trials combining FGFR and EGFR inhibitors have yet been initiated.

Histologic changes characteristic of epithelial-to-mesenchymal transition (EMT) occur in a subset of EGFR mutant NSCLC patients who develop acquired resistance to EGFR inhibitors, either independently or together with genetic resistance mechanisms such as $EGFR^{T790M}$ (8, 16, 17). Testing for changes in gene or protein expression indicative of EMT in patients is not routinely performed, so the incidence of this resistance mechanism may be underestimated. EMT has been associated with resistance to multiple anti-cancer drugs with varied mechanisms of action, including targeted therapies (16, 18, 19) and chemotherapy (20, 21). In addition, gene expression changes indicative of an emerging EMT have been observed in cells entering a drug tolerant "persister" state— a reversible phenotype characterized by reduced drug sensitivity, suppressed cell proliferation, and a chromatin remodeled state that was first described by the Settleman group (22). These drug tolerant persister cells may subsequently acquire $EGFR^{T790M}$ or other drug resistance mutations (23). Indeed, while select prior studies have reported strategies for targeting mesenchymal drug resistant cells *in vitro* (12, 22, 24), it remains unclear whether the *in vivo* microenvironmental drivers of EMT may be overcome by successful *in vitro* approaches, or whether it is possible to *prevent* EMT-mediated drug tolerance rather than targeting resistant clones once they have already completed an EMT.

In this study, we identify strategies to prevent EMT-mediated drug tolerant cells from surviving and giving rise to resistant clones. Whole genome CRISPR screening of fully mesenchymal EGFR mutant NSCLC cell lines derived from patient biopsies at the time of clinical progression—our clinical surrogate of persister cells – identified FGFR1 to be the top genomic mediator of resistance to third-generation EGFR TKIs. To our knowledge, this represents the first unbiased study of the dependencies of mesenchymal populations in EGFR-mutant NSCLC. Furthermore, we analyzed epithelial, drug sensitive cells as they begin to develop mesenchymal and drug-tolerant features. Dual EGFR + FGFR blockade (using an FGFR inhibitor that has been used in clinical trials (25, 26)) synergistically

decreased cell viability of mesenchymal patient-derived resistant cells (including those with a concurrent EGFR^{T790M} mutation), inhibited the long-term expansion of drug tolerant persister cells with mesenchymal features in vitro, and suppressed the development of acquired drug resistance in a xenograft mouse model over four months. These results reveal targetable dependencies of resistant, EGFR mutant lung cancer cells with mesenchymal features and suggest that dual EGFR + FGFR inhibition may be a successful clinical strategy for blocking and/or overcoming EMT-associated resistance.

Results

FGFR1 mediates resistance of mesenchymal EGFR^{T790M} cell lines to third generation EGFR inhibitors

To facilitate an unbiased genetic study, we characterized mesenchymal, EGFR-mutant NSCLC cell lines generated from patients who progressed on EGFR inhibition to find targets that may prevent the emergence of drug tolerant persister cells undergoing EMT-like transcriptional changes. We hypothesized that these mesenchymal resistant models may serve as surrogates for persister populations that also have a mesenchymal phenotype. We noted a clear mesenchymal phenotype that overlapped with the EGFR^{T790M} gatekeeper mutation in a subset of cases (Supplemental Figure 1A, Supplemental Table 1). Mesenchymal cell lines were insensitive to the third-generation EGFR inhibitor EGF816, even when harboring EGFR^{T790M} (Supplemental Figure 1B), consistent with prior observations that EMT can confer resistance to EGFR inhibitors (8, 15). Although EGF816 treatment led to dose dependent inhibition of EGFR phosphorylation in both epithelial and mesenchymal cell lines, downstream ERK signaling was not suppressed in mesenchymal cells (Supplemental Figure 1C), suggesting that these cells may utilize alternate inputs to the MAPK pathway for survival.

To identify a strategy to re-sensitize mesenchymal cell lines to EGFR inhibition, we performed whole genome CRISPR screening on two resistant patient-derived mesenchymal cell lines (Figure 1A). Cell lines were first engineered to stably-express Cas9 and then infected with a whole genome CRISPR library containing 10 guides per gene. Infected cells were cultured in the absence or presence of 100 nM EGF816 over a ten-day period, then harvested for sequencing of CRISPR sgRNA guides. We searched for genes which, when knocked out, caused selective depletion of cells in EGF816-treated versus untreated cells, indicating that gene function was required for cell survival in the presence of drug. FGFR1 was the top genomic target for re-sensitizing cells to EGF816 (Figure 1B). Other FGFR family members were not hits in these cell lines. FGFR1 knockout synergy in these mesenchymal cell lines aligned with high baseline expression of both FGFR1 and FGF2 (the ligand for FGFR1–4) (Figure 1C). The association between mesenchymal status and FGFR1, FGF2 expression was also observed in additional cell lines, including the large collection of CCLE lung cell lines (27) and an independent collection of nine EGFR mutant NSCLC cell lines derived from TKI-resistant patients generated at our institution that were not evaluated in the CRISPR screen (Supplemental Figure 2, Figure 1D).

To determine whether pharmacologic inhibition of FGFR1 is able to re-sensitize resistant mesenchymal EGFR mutant NSCLC cells to EGFR inhibitors, we treated cell lines with the

combination of EGF816 and the FGFR1/2/3 inhibitor BGJ398 (infigratinib) (28) in an 8×8 matrix format and assessed the effect on cell viability. A synergistic association between EGF816 and BGJ398, as determined by the Loewe excess additivity model (29), was observed over a range of doses to both slow proliferation and induce cell death in mesenchymal, but not in epithelial patient-derived cell lines (Figure 2A). EGF816 suppressed EGFR Y1068 phosphorylation and increased phosphorylation of FRS2a (an adaptor protein that plays a critical role in FGFR signaling), consistent with feedback activation of FGFR signaling upon EGFR pathway blockade (Figure 2B). Addition of BGJ398 to EGF816 led to a reduction of FRS2a phosphorylation in a dose-dependent manner, resulting in a reduction of ERK1/2 phosphorylation. Taken together, these results demonstrate that FGFR1 signaling facilitates the survival of mesenchymal-like, resistant EGFR mutant NSCLC cells upon EGFR blockade, and suggest that targeted inhibition of FGFR signaling can re-sensitize mesenchymal *EGFR* mutant cancers to EGFR inhibition. These results strengthen prior studies that point to the role of FGFR signaling in resistance to EGFR inhibitors (Azuma et al., 2014; Terai et al., 2013; Ware et al., 2013; Ware et al., 2010) by demonstrating that 1) FGFR1 is a *top* genomic strategy for re-sensitizing resistant cells to EGFR inhibition and, most importantly, 2) FGFR signaling is critical in patient-derived models of mesenchymal, drug tolerant cells.

Drug tolerant EGFR mutant NSCLC cells exhibit mesenchymal properties and increased expression of FGFR3

Previous work from our laboratory demonstrated that genetic mechanisms of resistance, such as $EGFR^{T790M}$, can evolve *de novo* during the course of therapy from drug tolerant persister cells with mesenchymal features, and that some mesenchymal features may be maintained after acquisition of $EGFR^{T790M}$ (23). We first confirmed that up-regulation of mesenchymal gene expression is a widespread feature of drug tolerant EGFR mutant NSCLC cell line models surviving prolonged drug treatment. We treated HCC827 and H1975 cells with gefitinib or the third-generation EGFR inhibitor WZ-4002 (H1975 cells harbor de novo $EGFR^{T790M}$), respectively, for two weeks and profiled gene expression in the surviving cells by RNA-seq (Figure 3A). In both models, gene set enrichment analysis revealed up-regulation of genes related to EMT in drug treated cells compared to untreated parental cells (Figure 3B, Supplemental Figure 3), similar to our prior findings in the PC9 cell line model (23). To validate these results, we determined the mRNA expression levels of canonical EMT-related or “stemness-related” genes after chronic EGFR TKI exposure in an expanded panel of EGFR mutant NSCLC cell lines (PC9, H1975, MGH119, HCC827) by quantitative RT-PCR. Although the exact expression profile of EMT-related transcription factors varied slightly between cell lines, we observed consistent up-regulation of the majority of EMT-related genes across the cell lines (Figure 3C).

We next examined whether FGF receptors were up-regulated in drug tolerant cells. In contrast to the fully resistant mesenchymal cell lines (Figure 1C), RNA-seq and quantitative RT-PCR analysis revealed that FGFR3 and, to a lesser extent FGFR2, were consistently up-regulated after two weeks of drug treatment (Figure 3D, E, Supplemental Figure 4). Additionally, we observed increased expression of multiple FGF ligands in drug tolerant cells (Figure 3D). To determine the kinetics of FGFR up-regulation, we treated H1975 and

HCC827 cells with EGFR inhibitor and assessed mRNA expression of FGFR3 and FGF2. Both FGFR3 and FGF2 were up-regulated within 24–72 hours of drug exposure (Supplemental Figure 4). These kinetics are consistent with previous studies that have reported up-regulation of FGFR3 signaling acutely after EGFR inhibitor treatment in specific models (11, 13).

FGFR3 is essential for the survival of EGFR mutant drug tolerant cells during EGFR inhibitor treatment

Several mechanisms that promote the survival of EGFR mutant drug tolerant "persister" cells have been proposed, including activation of IGF1R signaling, chromatin remodeling, and mesenchymal changes (22, 23). To evaluate a causal role for FGFR3 in promoting the survival of mesenchymal-like drug tolerant cells, we performed a pooled lentiviral shRNA dropout mini-screen targeting 75 genes with potential relevance to drug tolerant cell survival, including EMT-related transcription factors, genes involved in chromatin modification, and receptor tyrosine kinases that may play a role in adaptive resistance (Figure 4A, Supplemental Table 2). PC9 cells were transduced with lentiviral shRNAs (ten hairpins per gene) and treated with either vehicle or the third-generation EGFR inhibitor osimertinib (AZD9291) for three weeks (Figure 4B). Sufficient cell numbers were used to ensure shRNA representation of >1,000 cells/hairpin in the population of surviving drug tolerant cells (based on neutral selection), which represents approximately 1% of the starting parental population. Because of the large number of cells required, we used osimertinib to prevent the rapid emergence of any rare pre-existing $EGFR^{T790M}$ clones that would likely be present within such a large pool of PC9 parental cells (23) and confound the analysis. shRNA abundances in drug treated cells relative to the starting population and cells treated with vehicle for three weeks were determined by next-generation sequencing. We sought hairpins which 1) were represented at very low abundance after osimertinib treatment, 2) exhibited a large difference in abundance between osimertinib and vehicle-treated cells, and 3) that demonstrated consistent results in two independent replicates. Both FGFR3 and vimentin were among the top four genes with the greatest relative hairpin depletion after osimertinib treatment, suggesting that FGFR3 is necessary for drug tolerant cell survival during EGFR inhibitor treatment (Figure 4C). Of note, we also observed relative depletion of IGF1R hairpins, in agreement with prior studies demonstrating a role for IGF1R in the survival of persistent PC9 drug tolerant cells (22).

To validate these findings with respect to FGFR, we knocked down FGFR1, FGFR2 and FGFR3 in PC9 and HCC827 cells and assessed cell survival during gefitinib treatment. In order achieve robust and comparable knockdown of each FGFR family member (Supplemental Figure 5A), we used siRNAs rather than shRNAs, because we were unable to achieve reproducible knockdown >50% of FGFR1 despite testing multiple shRNAs. Consistent with the results of the shRNA screen, knockdown of FGFR3, but not FGFR1 or FGFR2, led to decreased survival of HCC827 and PC9 cells during gefitinib treatment (Figure 4D, Supplemental Figure 5B). In PC9 cells, two out of three FGFR1 siRNAs resulted in increased cell survival during gefitinib treatment, although this was not observed in HCC827 cells. Together, these results demonstrate that FGFR3 is necessary for supporting the survival of EGFR mutant drug tolerant cells during EGFR inhibitor treatment.

FGFR inhibition prevents the outgrowth of drug tolerant cells treated with EGFR inhibitors

Given the evidence suggesting a role for chromatin remodeling, mesenchymal gene expression and FGFR3 signaling in the survival of drug tolerant persister cells, we sought to identify pharmacological approaches that target these processes to prevent the outgrowth of drug tolerant clones. Based on our prior work, we hypothesize that targeting persister populations has the potential to prevent the development of acquired drug resistance (23). To our knowledge, prior studies have not determined if a drug combination may suppress persister cell growth in multiple cell lines over the timescales (i.e., several weeks) necessary to appreciate the emergence of EGFR inhibitor-resistant clones.

We labeled PC9, HCC827, H4006, and H1975 with red-fluorescent protein (RFP) and treated them with gefitinib or WZ4002 (a third generation EGFR TKI that targets the $EGFR^{T790M}$ mutation that is present in H9175 cells) for H1975 cells in the absence or presence of 17 different drugs (Supplemental Table 3) selected for their ability to modulate epigenetic pathways or other targets relevant to drug tolerance (Figure 5A). We included two FGFR inhibitors: BGJ398 and dovitinib. Surviving cells were quantified over a period of eight weeks using high content imaging. This time period encompassed the duration of initial drug response and the subsequent emergence of drug tolerant clones. An 100-fold range of concentrations was tested for each drug in order to account for differences in drug potency and define dosing limits above which growth suppression was due to single agent activity. We identified multiple drugs that suppressed the emergence of drug tolerant clones when combined with EGFR inhibitor in different cell lines (Figure 5B, Supplemental Figure 6A). For instance, the previously reported combination of IGF1R (AEW541) + EGFR inhibitors was effective in PC9 cells, but not in the other cell lines (Supplemental Figure 6B). In contrast, the pan-FGFR inhibitor BGJ398, when combined with EGFR inhibitors, consistently suppressed the emergence of drug tolerant clones in all cell lines examined (Figures 5B, C). The pan-FGFR inhibitor, Dovitinib (also known as Chir258), in combination with an EGFR TKI, also suppressed the outgrowth of persister cells in three out of four cell lines examined (Supplementary Figure 6C). We then replicated these findings in four cell lines in an independent experiment in which cell viability was tracked over time using a non-toxic, live-cell bioluminescent assay (Promega RealTime-Glo; Supplemental Figure 6). These results suggest that dual EGFR + FGFR inhibition may be a promising strategy for preventing the emergence of resistant clones.

To further establish the potential of combination EGFR + FGFR inhibitors to delay or prevent the development of acquired resistance, we treated multiple pools of HCC827 cells with gefitinib, BGJ398, or the combination and monitored for the development of acquired resistance. We chose to use the first-generation inhibitor gefitinib for this study as HCC827 cells have previously been shown to preferentially develop MET amplification rather than T790M as a mechanism of resistance to EGFR inhibitor therapy pathway (7, 30–32). Similar to what we observed in our previous experiments, all gefitinib-treated pools initially responded to treatment but then drug tolerant clones rapidly emerged (Figure 5D). Combined gefitinib + BGJ398 treatment suppressed the emergence of these drug tolerant clones, although we did observe the eventual emergence of resistance in two out of twenty pools. Both of these clones exhibited up-regulation of MET gene expression (Supplemental

Figure 7), consistent with the emergence of rare pre-existing MET-amplified clones that have been previously demonstrated to exist in the HCC827 cell line (33, 34). Taken together, these results strongly support the notion that dual EGFR + FGFR inhibition suppresses the emergence of drug tolerant persister clones in multiple models of EGFR-mutant NSCLC.

To understand the molecular basis for the suppression of drug tolerant cells by FGFR inhibition, we examined downstream MAPK signaling in HCC827 and PC9 cell lines. Gefitinib treatment acutely suppressed phospho-EGFR and phospho-ERK in both cell lines (Figure 5E). After prolonged gefitinib treatment, corresponding to the selection of drug tolerant cells, phospho-ERK was reactivated despite sustained inhibition of phospho-EGFR. This reactivation of phospho-ERK was suppressed in cells treated with the combination of gefitinib + BGJ398, consistent with FGFR-mediated reactivation of MAPK signaling in drug tolerant cells. Supporting this finding, we observed a rebound in DUSP6 (Dual Specificity Phosphatase 6, a transcriptional target and negative regulator of ERK) transcription in PC9 and HCC827 cells after prolonged gefitinib treatment, which was suppressed with the addition of BGJ398 (Figure 5F). To corroborate these findings, we treated H1975 cells with EGF816 alone or in combination with BGJ398 and assessed protein phosphorylation by ELISA. After EGF816 treatment, phosphorylation of both EGFR and ERK was initially suppressed (Supplemental Figure 8). At longer timepoints, despite continued inhibition of phospho-EGFR, there was rebound of phosphorylation of ERK, which coincided with an increase in phosphorylation of FGFR3. Combination treatment with EGF816 + BGJ398 blocked the activation of phospho-FGFR3 and led to sustained inhibition of phospho-ERK. These data reveal that dual EGFR + FGFR blockade inhibits the survival and outgrowth of mesenchymal-like drug tolerant clones by suppressing FGFR3-mediated reactivation of MAPK signaling.

Combination EGFR + FGFR inhibitors suppress the development of resistance in vivo

To investigate whether combined EGFR + FGFR inhibition may suppress the development of resistance *in vivo*, we established PC9 subcutaneous xenograft tumors in immunodeficient mice. We then treated mice with PC9 xenograft tumors with geftinib, BGJ398, or the combination for four months to assess both the initial response as well as the subsequent development of acquired resistance in each cohort (Figure 6A). As expected, gefitinib treatment led to initial tumor regression of approximately 60% after 21 days (Figure 6B, C). Treatment with the combination of gefitinib + BGJ398 led to an equivalent initial tumor regression (BGJ398 alone had no effect on tumor growth - data not shown). After prolonged treatment, gefitinib treated tumors began to develop resistance, with 8 of 9 progressing by 120 days of treatment (Figure 6C, D). In striking contrast, none of the tumors treated with gefitinib + BGJ398 showed any signs of progression after 120 days. We performed further analysis of five gefitinib-resistant tumors that had regrown to baseline volume and did not observe either $EGFR^{T790M}$ or MET amplification (Supplemental Figure 9), making it unlikely that resistance was caused by outgrowth of pre-existing resistant $EGFR^{T790M}$ or MET-amplified clones (23, 33).

Discussion

EMT has been observed in EGFR mutant NSCLCs at the time of acquired resistance and has also been associated with the survival of drug tolerant clones prior to the development of genetic resistance mechanisms (8, 16, 23). FGFR upregulation has also been reported as a short term response to EGFR inhibition in established cell line models (9–13). In this study, we use mesenchymal cells derived from patients at the time of progression on EGFR inhibitors as surrogates for the drug tolerant persister state and show that FGFR1 signaling is the top genomic strategy for resensitizing these cells to EGFR inhibitors. Synergy between the third generation EGFR inhibitor EGF816 and the FGFR inhibitor BGJ398 was observed in mesenchymal but not epithelial models, consistent with a specific dependence of mesenchymal EGFR mutant resistant cells on FGFR1 signaling. These results suggest a therapeutic strategy for resensitizing resistant EGFR mutant NSCLCs that have undergone EMT, including cancers that also harbor $EGFR^{T790M}$ and may not be sensitive to third generation EGFR inhibitors alone.

Complimenting this finding, we show that FGFR signaling is necessary for survival of epithelial, drug sensitive cells undergoing EMT-like changes during initial exposure to EGFR inhibitors. Interestingly, FGFR3 rather than FGFR1 is essential for cell survival in this context. Previous studies have demonstrated that EGFR inhibition leads to up-regulation of FGFR2 and 3 and that ligand-mediated activation of FGFR signaling protects cells from EGFR inhibitor treatment (13). Our studies extend these observations to show that up-regulation of both FGFR3 and FGF ligands is sustained in EGFR mutant drug tolerant cells that survive EGFR inhibitor therapy, leading to re-activation of ERK signaling despite continued inhibition of EGFR over long time periods. Most importantly, we show that dual FGFR + EGFR blockade prevented ERK reactivation that occurred after long-term EGFR inhibitor therapy and consistently suppressed the outgrowth of drug tolerant clones in multiple EGFR mutant cell line models in vitro, indicating that FGFR signaling is essential for the emergence of mesenchymal-like drug tolerant clones. Finally, we demonstrate that dual targeting of EGFR and FGFR inhibits the development of drug resistance *in vivo*. This *in vivo* proof of concept is particularly relevant to the study of EMT, an epigenetic phenomenon that is highly influenced my microenvironmental cues. We also examined several drugs that target epigenetic modulators but only observed sporadic activity of different drugs in different cell lines. Of note, a recent study revealed that ZEB1-mediated suppression of BIM can blunt the apoptotic response of mesenchymal cancers to TKI therapy (35), indicating that multiple mechanisms may contribute to the lack of efficacy of EGFR inhibitors in mesenchymal cancers. Overall, these data suggest that dual EGFR + FGFR inhibition may also be a promising long-term therapeutic strategy for preventing the survival of drug tolerant clones in the setting of EMT-related adaptive resistance.

Our findings add to a growing body of evidence converging on the central importance of FGFR signaling in the survival of mesenchymal cells. Recently, FGFR1 was implicated in the intrinsic resistance of mesenchymal KRAS mutant NSCLCs to MEK inhibitors (18, 36). However, FGFR inhibition did not sensitize epithelial KRAS mutant cancers to MEK inhibition. FGFR1 over-expression has been shown to decrease sensitivity to EGFR TKIs pre-clinical models and be associated with decreased response to EGFR TKI therapy in

EGFR mutant NSCLC patients (37). FGFR1 dependency has also been observed in cell line models of acquired resistance to EGFR inhibitors (10, 12, 13). In these studies, resistant cells lost dependency on EGFR and became sensitive to FGFR inhibition alone (Ware et al., 2013), or were only treated with EGFR inhibitor for very short time periods to assess acute response of FGFR inhibitors rather than potential effects on persister cell development (10). In our study, the mesenchymal resistant patient-derived cell lines generated from EGFR mutant NSCLCs at the time of clinical acquired resistance were not sensitive to FGFR inhibition alone, arguing against a case of simple oncogene switching, but the combination of EGFR and FGFR inhibitors overcame resistance when neither alone was sufficient.

Our results suggest that different FGFR family members may be involved in bypassing EGFR inhibition depending on context. Very early after initiation of EGFR inhibitor treatment, FGFR3 is up-regulated and plays a dominant role during the selection of mesenchymal-like drug tolerant clones. In fully mesenchymal resistant cells, FGFR1 appears to be critical for cell survival. Given the limited number of models available for study, it is difficult to make a definitive conclusion about whether this distinction is strictly followed during evolving resistance. The role of FGFR1 is supported by other studies demonstrating that FGFR1 expression is up-regulated in mesenchymal cancers, such as bladder cancer, and FGFR1 knock-down alters expression of EMT-related transcription factors (38). These results, together with the observation that the mesenchymal versus epithelial phenotype correlates with FGFR1 expression among CCLE cell lines and a set of our patient-derived EGFR-mutant NSCLC cell lines, suggests that FGFR1 is a key survival factor in mesenchymal cells across different tissue origins. Our results suggest that up-regulation of FGFR3 may play a similar role in the survival of drug tolerant cells which have not yet developed a fully mesenchymal phenotype. We observed that this process occurs within 24 hours, more rapidly than the up-regulation of mesenchymal transcription factors (23). This time frame is relatively short to achieve either a phenotypic shift to the mesenchymal state or significant selection of pre-existing mesenchymal sub-clones. These results are most consistent with a model in which FGFR3 induction is an early direct effect of EGFR inhibition, and it is possible that cells that engage this pathway may be predisposed to embark on an EMT.

Since lung cancers may be heterogeneous populations of sensitive, drug tolerant, and resistant clones at varying stages along the EMT continuum during the course of EGFR inhibitor therapy, it is possible that both FGFR family members might be operational at the same time within a given tumor. Many studies have revealed the complexity of FGFR signaling, which can result from differences in both the intrinsic signaling properties of FGFR family members as well as the specific FGF ligands available, suggesting non-redundant functionality between FGFR family member (39–42). For instance, FGFR3 has been shown to transduce a different signal that either inhibits or stimulates cell proliferation depending on the cell type (43–45). FGFR3 has greater ligand independent dimerization than FGFR1; moreover, FGF1 and FGF2 induce different kinase domain conformations of FGFR3 (46). Several studies have shown that FGFR3 does not contain 3 of the 7 phosphorylation sites in the kinase domain of FGFR1, including the Y463 CRKL binding site, which facilitates FRS2a activation (47–49). It is possible that increased expression of FGFR3 leading to ligand-independent FGFR3 survival signaling and FGF ligand-driven

activation of FGFR1 could play complementary roles in engaging different intracellular signaling as cells evolve along a mesenchymal trajectory. Of note, our in vitro studies do not account for any potential contribution of FGF signaling from the tumor micro-environment, which might be important in patients. From this perspective, a pan-FGFR inhibitor such as BGJ398 might be attractive because it would be effective regardless of whether one or more FGFR family members may be dominant in a given context. The future development of selective FGFR inhibitors will provide the opportunity to directly test the efficacy of selective inhibition of individual FGFR family members.

A number of studies have shown that alternate receptor tyrosine kinase signaling can contribute to both intrinsic and acquired resistance to targeted therapies by activating downstream effectors that are redundant with the therapeutically inhibited pathway (7, 30–32). In these cases, dual-RTK inhibition may be an attractive approach for overcoming or preventing drug resistance. One challenge in developing clinically useful therapeutic strategies, however, is the potential heterogeneity of bypass signaling pathways that may occur even in the same cancer sub-type. For instance, previous studies have reported that drug tolerant PC9 cells are dependent on IGF1R for survival during EGFR inhibitor treatment (22); we confirmed this in PC9 cells but did not observe this dependency in any of the other EGFR mutant NSCLC models that we investigated.

To our knowledge, this is the first work demonstrating *in vivo* efficacy of a drug combination in targeting persister cells in EGFR-mutant NSCLC. Along with the whole genome screening results in patient-derived cell lines implicating FGFR1 signaling in maintenance of drug tolerance in mesenchymal cells, this work demonstrates that dual EGFR-FGFR blockade is capable of inhibiting the development of acquired resistance *in vivo* and may have potential to block the evolution of EMT-associated acquired resistance in EGFR mutant NSCLC. We hope this work provides the preclinical evidence required to begin a clinical trial testing upfront combination therapy with EGFR and FGFR inhibitors among EGFR-mutant NSCLC patients.

Methods

Cell lines

Human EGFR mutated NSCLC cell lines used: PC9 [EGFR exon 19 delE746-A750], HCC827 (EGFR exon 19 delE746-A750), HCC4006 (exon 19 delL747-A750, P ins), H1975 [EGFR L858R,T790M], MGH707–1 (EGFR exon 19delE746-A750, T790M), MGH174–2A (EGFR exon 19delE746-A750), MGH721–1(EGFR exon 19delE746-A750, T790M), MGH792–1A (EGFR L858R) and MGH700–2D (EGFR exon 19delE746-A750). Commercially available cell lines were obtained from the Center for Molecular Therapeutics at MGH, where cell line identity has been authenticated by STR analysis (Bio-synthesis, Inc). Patient-derived cell lines were established in our laboratory from core biopsy or pleural effusion samples as previously described (10). All patients signed informed consent to participate in a Dana-Farber–Harvard Cancer Center Institutional Review Board–approved protocol giving permission for research to be performed on their samples. Cell lines were cultured in RPMI-1640 growth medium, supplemented with 10% FBS and 1% P/S at 37C in

a humidified 5% CO2 incubator. All cells were verified to be free of mycoplasma contamination.

Antibodies and reagents

The following antibodies were used: phospho EGFR Y1068 (Abcam AB5644), phospho EGFR Y1068 (Cell Signaling 3777), EGFR (Cell Signaling 2646), EGFR (Cell Signaling 4267), phospho ERK1/2 T202/Y204 (Cell Signaling 9101), phospho ERK1/2, T202/Y204 (Cell Signaling 4370), ERK1/2 (Cell Signaling 9102), phospho AKT S473 (Cell Signaling 4060), AKT1/2/3 (Santa Cruz sc-8312), BIM (Cell Signaling 2933), Actin (Cell Signaling 4970), Actin-HRP conjugated (Cell Signaling 12262), FGFR1 (Cell Signaling 9740), and FGFR3 (Cell Signaling 4574), phospho FRS2α Y436 (Cell Signaling 3861), E-Cadherin (Cell Signaling 3195), N-Cadherin (Cell Signaling 13116), Zeb1 (Cell Signaling 3396), Vimentin (Cell Signaling 5741). Gefitinib, WZ4002, AZD9291, and BGJ398 (all from Selleck) were dissolved in DMSO to a final concentration of 10 mmol/liter and stored at −20 °C. The 18 drugs tested in the long-term assay are listed in Supplemental Table 3.

CRISPR Screen

Cells were transfected with a Cas9 containing vector using the EF1alpha-long promoter. Cas9 positivity was verified by flow cytometry and cell populations expressing 70% Cas9 or higher were expanded for the screen. For each library pool in the screen, cells were plated in 5-layer CellSTACK flasks (Corning, EK-680940) at predetermined densities based on doubling time and sensitivity to EGF816, with a minimum of 80×106 cells per flask. Cells were transduced with the screen virus pools containing the CRISPR guides in 500mL media containing 8μg/mL polybrene (EMD Millipore). Cells were then put under puromyocin selection for 72 hours. Prior to EGF816 treatment, transduction efficiency was confirmed by RFP expression using flow cytometry. Cell populations that expressed more than 90% RFP were then treated for 10 days with or without EGF816 at a dose equivalent to the IC90 in each cell line. After 10 days, cells were trypsinzied, pelleted to 100×10^6 cells, and DNA was extracted using Qiagen DNA maxi kit. DNA samples were checked by PCR before being submitted for downstream sequencing to determine the proportional representation of the CRISPR guides.

8×8 Combination Proliferation Assay

Cells were seeded at a density of 3000 cells/well in black clear bottom 96 well plates (Corning, 3904), and allowed to attach overnight. An 8×8 matrix of two compound titrations were mixed in DMSO, diluted into media, then added to cells giving a final DMSO concentration of 0.1%. Cells were cultured for 3 days, prior to addition of Cell Titer GLO reagent. Patient-derived cell lines were cultured for 7 days prior to addition of Cell Titer GLO reagent.

Long term drug assay

Cells were seeded at a density of 5,000 cells/well in black, clear bottom 96 well plates. After 24 hours, cells were drugged and maintained with biweekly media changes. Cell count was

calculated at 24h post-seeding and every 3–7 days thereafter, using High Content Imaging or Promega RealTime Glo.

High-content imaging and image analysis

Imaging of the immunofluorescence-stained cultures was performed with Molecular Devices' Image Express Micro high-content imager. Briefly, the post-laser z-offset was determined for correct autofocusing, and the exposure time for each illumination filter was calculated. Several wells across the 384-well plate were tested for consistency prior to acquisition of the entire plate. Analysis of the fluorescent images was done with Molecular Devices' MetaExpress software and their Multi-wavelength Cell Scoring application. The minimum and maximum width as well as the signal intensity above local background were determined for proper segmentation of the nuclear Hoechst 33342 stain and the cytoplasmic CK8/18 stain (entire cell). Several wells of the 384-well plate were previewed by eye for accurate segmentation prior to analysis of the entire plate. Data collected from the analysis included the number of total cells (Hoechst 33342-positive nuclei count), the number of epithelial cells (Hoechst 33342-positive and CK8/18-positive cell count) and the number of non-epithelial cells (Hoechst 33342-positive and CK8/18-negative cell count).

RealTime Glo viability assay

A non-cytotoxic, bioluminescence-producing assay was used according to the manufacturer's instructions (Promega). Luminscence at 570nm was recorded. Triplicate values were averaged in Microsoft Excel and graphed in Prism. Twice weekly media change immediately followed reading of luminescence.

3×3 Mechanistic Studies

Patient-derived cell lines were seeded into 6 well plates at a density of 500,000 cells/well, and allowed to attach overnight. A 3×3 combination grid was selected based on proliferation results, compounds then incubated on cells for 24 hours. Cells were washed once with PBS, then lysed on ice using MSD Tris Lysis Buffer (Mesoscale R60TX-2), complete with protease inhibitor cocktail (Sigma P8340), phosphatase inhibitor cocktail 2 (Sigma P5726), phosphatase inhibitor cocktail 3 (Sigma P0044) for 10 minutes with scraping. Lysates were collected, micro-centrifuged at 4°C and quantified for total protein by BCA assay (Pierce Cat#23225).

Western blotting

Lysates were prepared for a western blot following the BCA assay, using 4X LDS Sample Buffer (Invitrogen NP0007), containing 1X Sample Reducing Agent (Invitrogen NP0009), heated at 95°C for 10 minutes. Samples were loaded into a 4–12% NuPAGE Bis Tris gel (Invitrogen WG1402BOX) and run using MOPS running buffer (Invitrogen NP0001). Proteins were transferred onto nitrocellulose using the BioRad Trans-Blot Turbo transfer system (Bio-Rad Cat#1704150). Membranes were blocked with Tris buffered saline containing 0.1% Tween 20 (w/v) (TBS-T) and 5% non-fat milk, for a minimum of 1 hour at room temperature on a rocking platform. Primary antibodies were used as directed by the manufacturer, incubated overnight at 4°C on a rocking platform. Secondary HRP linked

antibodies (anti-mouse HRP CST#7076, anti-rabbit HRP CST#7074) were used where appropriate, incubated in TBS-T 5% MILK, for a minimum of 1 hour at room temperature on a rocking platform. Membranes were visualized using SuperSignal West Femto Maximum Sensitivity Substrate (ThermoFisher Cat#34095).

NanoString RNA analysis

Cell lines (HCC827 and NCI-H1975) were treated with IC70 doses of EGF816 over a five day time course. Samples were collected at 4, 24, 72, 120 hours post treatment and RNA was extracted using the Qiagen RNeasy Mini Kit (Qiagen Cat#74104). RNA was normalized to 100ng in 10μl and hybridized to the 200-gene Nanostring PanCancer panel (Nanostring Cat#XT-CSO-PATH1–12) according to the manufacturers instructions. The samples were run on the nCounter prep station and scanned at 600 scans per chip. Data was analyzed using the nSolver software (https://www.nanostring.com/products/analysis-software/nsolver) and all counts were normalized to both housekeeping genes and internal controls provided in the codeset.

RNA sequencing

Profiling of drug tolerant cells: Cell lines (PC9, HCC827 and HCC4006) were drugged with 300 nM Gefitinib or 1 μM WZ4002 (H1975) for two weeks. Extraction of mRNA from biological triplicates of drugged and parental cells was performed using the Qiagen RNeasy kit. RNAseq libraries were constructed from polyadenosine (polyA)-selected RNA using the NEBNext Ultra Directional RNA library prep kit for Illumina (New England BioLabs) and sequenced on an Illumina HiSeq2500 instrument. STAR aligner51 was used to map sequencing reads to transcripts in the human hg19 reference genome. Read counts for individual transcripts were produced with HTSeq-count52, followed by the estimation of expression values and detection of differentially expressed transcripts using a custom R script. Gene-set enrichment analysis (GSEA) software was used to analyze the enrichment of functional gene groups among differentially expressed transcripts.

Baseline expression profiling of patient-derived cell lines: Total RNA was separately extracted and quantified using the Agilent RNA 6000 Nano Kit (catalog number 5067–1511) on the Agilent 2100 BioAnalyzer. 200ng of high purity RNA (RNA Integrity Number 7.0 or greater) was used as input to the Illumina TruSeq Stranded mRNA Library Prep Kit, High Throughput (catalog number RS-122–2103), and the sample libraries were generated per manufacturer's specifications on the Hamilton STAR robotics platform. The PCR amplified RNA-Seq library products were then quantified using the Advanced Analytical Fragment Analyzer Standard Sensitivity NGS Fragment Analysis Kit (catalog number DNF-473). The samples were diluted to 10 nM in Qiagen Elution Buffer (Qiagen material number 1014609), denatured, and loaded at a range of 2.5 to 4.0 pM on an Illumina cBOT using the HiSeq® 4000 PE Cluster Kit (catalog number PE-410–1001). The RNA-Seq libraries were sequenced on a HiSeq® 4000 at 75 base pair paired end with 8 base pair dual indexes using the HiSeq® 4000 SBS Kit, 150 cycles (catalogue number FC-410–1002). The sequence intensity files were generated on instrument using the Illumina Real Time Analysis software. The resulting intensity files were demultiplexed with the bcl2fastq2 software and aligned to the human transcriptome using PICSES.

Gene expression of drug tolerant cells by quantitative RT-PCR

Cells were treated with drugs for two weeks and RNA was extracted using the RNeasy Kit (Qiagen). cDNA was prepared from 500 ng total RNA with the First Strand Synthesis Kit (Invitrogen) using oligo-dT primers. Quantitative PCR was performed using FastStart SYBR Green (Roche) on a Lightcycler 480. Unless otherwise indicated, mRNA expression relative to the geometric mean of three housekeeping gene (b-actin, RPS9, GAPDH) was calculated using the delta-delta threshold cycle (ΔΔCT) method. Primer sequences are listed in Supplemental Table 4.

shRNA dropout screen

A list of 75 genes related to chromatin modification, EMT, or known EGFR-TKI resistance mechanisms was compiled (Supplemental Table 2). The set of chromatin modifying genes were compiled previously (50). Bacterial clones for ten shRNAs per gene were acquired from the Broad RNAi consortium and pooled at equal optical densities. Pooled shRNAs were prepped and viral production was achieved in 293T cells. Next-generation sequencing confirmed the broad distribution of hairpins. 100 million PC9 cells were infected with the viral pool, and puromycin selection at an MOI of ~0.1 was completed. The surviving cells were expanded for seven doublings. 100 million cells were drugged with AZD9291 for 21 days, after which time roughly 1 million cells survived (this population size was chosen to ensure > 1,000 cells/hairpin after drug selection). 10 million cells were drugged with vehicle for 21 days, and every plate split from this cohort was saved. Another 10 million cells were frozen at t0. DNA was harvested from all specimens together using the Qiagen Blood Midi Kit. Genomic DNA concentrations were measured using a Picogreen dye-binding assay giving a typical yield of 1μg gDNA per million cells. For Next Generation Sequencing (NGS) library generation, the pooled shRNA sequences were PCR amplified in 8 independent 100 μL PCR reactions using 1 μg of input gDNA per reaction with Titanium Taq, a single forward primer and one of 8 indexing oligos for 30 cycles. All 8 independent PCR reactions were pooled and purified using the Agencourt AMPure XP PCR cleanup kit (Beckman Coulter). The resulting products were quantified using the Advanced Analytical Fragment Analyzer. Individual shRNA sequence representation was measured on the Illumina MiSeq platform. For good representation of each shRNA in the NGS data, ~1 million raw Illumina sequence reads were generated per sample averaging approximately > 1000 reads per shRNA. Note that the individual plasmid pool for this shRNA library was spiked into the MiSeq flowcell at 15% of the total loading volume as a normalization control. The resulting sample data were demultiplexed using the bcl2fastq script, and the resulting fastq files aligned to a reference file of all shRNAs in the pool using the CASAVA 1.8.2 software. The resulting counts were then normalized to a fixed number of reads, and a small constant was added to remove all zero counts in the data. These normalized count data were then compared in the 3 week untreated and 3 week AZD9291 treated condition across all shRNAs for sequence drop outs.

siRNA validation of FGFR knockdown

Cell lines were transfected with 50nmol/L of siRNA using Lipofectamine RNAi MAX (Invitrogen) according to manufacturer's instructions. siRNA sequences are shown in

Supplemental Table 5. The day after transfection (day 2), cells were seeded for the viability assays or RNA extraction. On day 3, cells were treated with gefitinib or vehicle. Cell viability was determined after 72 hours of drug treatment using CellTiter-Glo viability assay (Promega) according to manufacturer's instructions. RNA was extracted after 24 hours of drug treatment using the RNeasy Kit (Qiagen). cDNA was prepared from 500 ng total RNA with First Strand Synthesis Kit (Invitrogen) using oligo-DT primers and quantitative PCR was performed using FastStart SYBR Green (Roche) on a Lightcycler 480. mRNA expression relative to the mRNA levels of the housekeeping gene β-actin was calculated using the delta-delta threshold cycle (ΔΔCT) method. Primer sequences are listed in Supplemental Table 4. Relative gene expression levels were determined at baseline (for FGFR1) or after gefitinib treatment (for FGFR2 and FGFR3, which were expressed at very low levels at baseline).

In vivo studies

Mouse work was conducted under Institutional Animal Care and Use Committee–approved animal protocols in accordance with institutional guidelines (MGH Subcommittee on Research Animal Care, OLAW Assurance A3596–01). For xenograft studies, cell line suspensions were prepared in 1:10 matrigel and 5×10^6 cells were injected subcutaneously into the flanks of female athymic nude (Nu/Nu) mice (6–8 weeks old). Visible tumors developed in approximately 2–3 weeks. Tumors were measured with electronic calipers and the tumor volume was calculated according to the formula $\text{Vol} = 0.52 \times L \times W^2$. Mice with established tumors were randomized to drug-treatment groups using covariate-adaptive randomization to minimize differences in baseline tumor volumes: Gefitinib at 6.25 mg/kg (polysorbate), BGJ398 at 30 mg/kg (sodium acetate), or combinations thereof. Drug treatments were administered by oral gavage and tumor volumes were measured twice weekly. Investigators performing tumor measurements were not blinded to treatment groups. Sample size (9 per treatment group) was chosen to verify satisfactory interanimal reproducibility.

Supplementary Material

Refer to Web version on PubMed Central for supplementary material.

Acknowledgements

We thank Dr. Rafael Irizarry and Irineo Cabreros for guidance in statistical analyses related to shRNA dropout screening. We also thank Drs. Cyril Benes, Daniel Haber, Joan Brugge, Kornelia Polyak, and Robert Weinberg for helpful discussions throughout the development of this work.

This study was funded by support from the NIH F30 CA213726-01A1 (S.R.), K08CA197389 (A.N.H.), R01CA137008 (L.V.S.), Doris Duke Charitable Foundation (A.N.H), Stand Up To Cancer (A.N.H. and L.V.S.), National Science Foundation (J.A.E.), V Foundation (J.A.E), Ludwig Cancer Research (A.N.H.), LungStrong and Be a Piece of the Solution.

Conflict of Interest: I.M., E.L., N.H., J.K., R.T., D.A.R., P.S.H., M.J.N., J.B. and J.A.E. are employees of Novartis, Inc., as noted in the affiliations. M.J.N. & J.A.E. hold equity interest in Novartis, Inc. A.N.H receives research support from Novartis, Amgen, Pfizer, and Relay Therapeutics. Z.P. is a consultant/advisory board member for Takeda, AstraZeneca, GuardantHealth and Novartis, and receives institutional research support from Novartis. L.V.S is a consultant for AstraZeneca, Boehringer-Ingelheim, Novartis, Pfizer, Genentech, Merrimack, and BMS.

References

1. Lynch TJ, Bell DW, Sordella R, Gurubhagavatula S, Okimoto RA, Brannigan BW, et al. Activating mutations in the epidermal growth factor receptor underlying responsiveness of non-small-cell lung cancer to gefitinib. N Engl J Med 2004;350(21):2129–39. [PubMed: 15118073]
2. Paez JG, Janne PA, Lee JC, Tracy S, Greulich H, Gabriel S, et al. EGFR mutations in lung cancer: correlation with clinical response to gefitinib therapy. Science 2004;304(5676):1497–500. [PubMed: 15118125]
3. Mok TS, Wu YL, Thongprasert S, Yang CH, Chu DT, Saijo N, et al. Gefitinib or carboplatin-paclitaxel in pulmonary adenocarcinoma. N Engl J Med 2009;361(10):947–57. [PubMed: 19692680]
4. Maemondo M, Inoue A, Kobayashi K, Sugawara S, Oizumi S, Isobe H, et al. Gefitinib or chemotherapy for non-small-cell lung cancer with mutated EGFR. N Engl J Med 2010;362(25): 2380–8. [PubMed: 20573926]
5. Kobayashi S, Boggon TJ, Dayaram T, Janne PA, Kocher O, Meyerson M, et al. EGFR mutation and resistance of non-small-cell lung cancer to gefitinib. N Engl J Med 2005;352(8):786–92. [PubMed: 15728811]
6. Pao W, Miller VA, Politi KA, Riely GJ, Somwar R, Zakowski MF, et al. Acquired resistance of lung adenocarcinomas to gefitinib or erlotinib is associated with a second mutation in the EGFR kinase domain. PLoS Med 2005;2(3):e73. [PubMed: 15737014]
7. Engelman JA, Zejnullahu K, Mitsudomi T, Song Y, Hyland C, Park JO, et al. MET amplification leads to gefitinib resistance in lung cancer by activating ERBB3 signaling. Science 2007;316(5827): 1039–43. [PubMed: 17463250]
8. Sequist LV, Waltman BA, Dias-Santagata D, Digumarthy S, Turke AB, Fidias P, et al. Genotypic and histological evolution of lung cancers acquiring resistance to EGFR inhibitors. Sci Transl Med 2011;3(75):75ra26.
9. Azuma K, Kawahara A, Sonoda K, Nakashima K, Tashiro K, Watari K, et al. FGFR1 activation is an escape mechanism in human lung cancer cells resistant to afatinib, a pan-EGFR family kinase inhibitor. Oncotarget 2014;5(15):5908–19. [PubMed: 25115383]
10. Crystal AS, Shaw AT, Sequist LV, Friboulet L, Niederst MJ, Lockerman EL, et al. Patient-derived models of acquired resistance can identify effective drug combinations for cancer. Science 2014;346(6216):1480–6. [PubMed: 25394791]
11. Terai H, Soejima K, Yasuda H, Nakayama S, Hamamoto J, Arai D, et al. Activation of the FGF2-FGFR1 autocrine pathway: a novel mechanism of acquired resistance to gefitinib in NSCLC. Mol Cancer Res 2013;11(7):759–67. [PubMed: 23536707]
12. Ware KE, Hinz TK, Kleczko E, Singleton KR, Marek LA, Helfrich BA, et al. A mechanism of resistance to gefitinib mediated by cellular reprogramming and the acquisition of an FGF2-FGFR1 autocrine growth loop. Oncogenesis 2013;2:e39. [PubMed: 23552882]
13. Ware KE, Marshall ME, Heasley LR, Marek L, Hinz TK, Hercule P, et al. Rapidly acquired resistance to EGFR tyrosine kinase inhibitors in NSCLC cell lines through de-repression of FGFR2 and FGFR3 expression. PLoS One 2010;5(11):e14117. [PubMed: 21152424]
14. Janne PA, Yang JC, Kim DW, Planchard D, Ohe Y, Ramalingam SS, et al. AZD9291 in EGFR inhibitor-resistant non-small-cell lung cancer. N Engl J Med 2015;372(18):1689–99. [PubMed: 25923549]
15. Jia Y, Juarez J, Li J, Manuia M, Niederst MJ, Tompkins C, et al. EGF816 Exerts Anticancer Effects in Non-Small Cell Lung Cancer by Irreversibly and Selectively Targeting Primary and Acquired Activating Mutations in the EGF Receptor. Cancer Res 2016;76(6):1591–602. [PubMed: 26825170]
16. Uramoto H, Iwata T, Onitsuka T, Shimokawa H, Hanagiri T, Oyama T. Epithelial-mesenchymal transition in EGFR-TKI acquired resistant lung adenocarcinoma. Anticancer Res 2010;30(7): 2513–7. [PubMed: 20682976]
17. Cardnell RJ, Feng Y, Diao L, Fan YH, Masrorpour F, Wang J, et al. Proteomic markers of DNA repair and PI3K pathway activation predict response to the PARP inhibitor BMN 673 in small cell lung cancer. Clin Cancer Res 2013;19(22):6322–8. [PubMed: 24077350]

18. Kitai H, Ebi H, Tomida S, Floros KV, Kotani H, Adachi Y, et al. Epithelial-to-Mesenchymal Transition Defines Feedback Activation of Receptor Tyrosine Kinase Signaling Induced by MEK Inhibition in KRAS-Mutant Lung Cancer. Cancer Discov 2016;6(7):754–69. [PubMed: 27154822]
19. Gainor JF, Dardaei L, Yoda S, Friboulet L, Leshchiner I, Katayama R, et al. Molecular Mechanisms of Resistance to First- and Second-Generation ALK Inhibitors in ALK-Rearranged Lung Cancer. Cancer Discov 2016;6(10):1118–33. [PubMed: 27432227]
20. Fischer KR, Durrans A, Lee S, Sheng J, Li F, Wong ST, et al. Epithelial-to-mesenchymal transition is not required for lung metastasis but contributes to chemoresistance. Nature 2015;527(7579): 472–6. [PubMed: 26560033]
21. Zheng X, Carstens JL, Kim J, Scheible M, Kaye J, Sugimoto H, et al. Epithelial-to-mesenchymal transition is dispensable for metastasis but induces chemoresistance in pancreatic cancer. Nature 2015;527(7579):525–30. [PubMed: 26560028]
22. Sharma SV, Lee DY, Li B, Quinlan MP, Takahashi F, Maheswaran S, et al. A chromatin-mediated reversible drug-tolerant state in cancer cell subpopulations. Cell 2010;141(1):69–80. [PubMed: 20371346]
23. Hata AN, Niederst MJ, Archibald HL, Gomez-Caraballo M, Siddiqui FM, Mulvey HE, et al. Tumor cells can follow distinct evolutionary paths to become resistant to epidermal growth factor receptor inhibition. Nat Med 2016;22(3):262–9. [PubMed: 26828195]
24. Viswanathan VS, Ryan MJ, Dhruv HD, Gill S, Eichhoff OM, Seashore-Ludlow B, et al. Dependency of a therapy-resistant state of cancer cells on a lipid peroxidase pathway. Nature 2017;547(7664):453–7. [PubMed: 28678785]
25. Goyal L, Saha SK, Liu LY, Siravegna G, Leshchiner I, Ahronian LG, et al. Polyclonal Secondary FGFR2 Mutations Drive Acquired Resistance to FGFR Inhibition in Patients with FGFR2 Fusion-Positive Cholangiocarcinoma. Cancer Discov 2017;7(3):252–63. [PubMed: 28034880]
26. Javle M, Lowery M, Shroff RT, Weiss KH, Springfeld C, Borad MJ, et al. Phase II Study of BGJ398 in Patients With FGFR-Altered Advanced Cholangiocarcinoma. J Clin Oncol 2018;36(3): 276–82. [PubMed: 29182496]
27. Barretina J, Caponigro G, Stransky N, Venkatesan K, Margolin AA, Kim S, et al. The Cancer Cell Line Encyclopedia enables predictive modelling of anticancer drug sensitivity. Nature 2012;483(7391):603–7. [PubMed: 22460905]
28. Guagnano V, Furet P, Spanka C, Bordas V, Le Douget M, Stamm C, et al. Discovery of 3-(2,6-dichloro-3,5-dimethoxy-phenyl)-1-{6-[4-(4-ethyl-piperazin-1-yl)-phenylamin o]-pyrimidin-4-yl} −1-methyl-urea (NVP-BGJ398), a potent and selective inhibitor of the fibroblast growth factor receptor family of receptor tyrosine kinase. J Med Chem 2011;54(20):7066–83. [PubMed: 21936542]
29. Loewe S The problem of synergism and antagonism of combined drugs. Arzneimittelforschung 1953;3(6):285–90. [PubMed: 13081480]
30. Wilson TR, Fridlyand J, Yan Y, Penuel E, Burton L, Chan E, et al. Widespread potential for growth-factor-driven resistance to anticancer kinase inhibitors. Nature 2012;487(7408):505–9. [PubMed: 22763448]
31. Katayama R, Shaw AT, Khan TM, Mino-Kenudson M, Solomon BJ, Halmos B, et al. Mechanisms of acquired crizotinib resistance in ALK-rearranged lung Cancers. Science translational medicine 2012;4(120):120ra17.
32. Isozaki H, Ichihara E, Takigawa N, Ohashi K, Ochi N, Yasugi M, et al. Non-Small Cell Lung Cancer Cells Acquire Resistance to the ALK Inhibitor Alectinib by Activating Alternative Receptor Tyrosine Kinases. Cancer Res 2016;76(6):1506–16. [PubMed: 26719536]
33. Turke AB, Zejnullahu K, Wu YL, Song Y, Dias-Santagata D, Lifshits E, et al. Preexistence and clonal selection of MET amplification in EGFR mutant NSCLC. Cancer Cell 2010;17(1):77–88. [PubMed: 20129249]
34. Bhang HE, Ruddy DA, Krishnamurthy Radhakrishna V, Caushi JX, Zhao R, Hims MM, et al. Studying clonal dynamics in response to cancer therapy using high-complexity barcoding. Nat Med 2015;21(5):440–8. [PubMed: 25849130]

35. Song KA, Niederst MJ, Lochmann TL, Hata AN, Kitai H, Ham J, et al. Epithelial-to-mesenchymal transition antagonizes response to targeted therapies in lung cancer by suppressing BIM. Clin Cancer Res 2017.
36. Manchado E, Weissmueller S, Morris JPt, Chen CC, Wullenkord R, Lujambio A, et al. A combinatorial strategy for treating KRAS-mutant lung cancer. Nature 2016;534(7609):647–51. [PubMed: 27338794]
37. Quintanal-Villalonga A, Molina-Pinelo S, Cirauqui C, Ojeda-Marquez L, Marrugal A, Suarez R, et al. FGFR1 cooperates with EGFR in lung cancer oncogenesis, and their combined inhibition shows improved efficacy. Journal of thoracic oncology : official publication of the International Association for the Study of Lung Cancer 2019.
38. Cheng T, Roth B, Choi W, Black PC, Dinney C, McConkey DJ. Fibroblast growth factor receptors-1 and −3 play distinct roles in the regulation of bladder cancer growth and metastasis: implications for therapeutic targeting. PLoS One 2013;8(2):e57284. [PubMed: 23468956]
39. Ornitz DM, Itoh N. The Fibroblast Growth Factor signaling pathway. Wiley Interdiscip Rev Dev Biol 2015;4(3):215–66. [PubMed: 25772309]
40. Zhou WY, Zheng H, Du XL, Yang JL. Characterization of FGFR signaling pathway as therapeutic targets for sarcoma patients. Cancer Biol Med 2016;13(2):260–8. [PubMed: 27458533]
41. Haugsten EM, Wiedlocha A, Olsnes S, Wesche J. Roles of fibroblast growth factor receptors in carcinogenesis. Mol Cancer Res 2010;8(11):1439–52. [PubMed: 21047773]
42. Moosa S, Wollnik B. Altered FGF signalling in congenital craniofacial and skeletal disorders. Semin Cell Dev Biol 2016;53:115–25. [PubMed: 26686047]
43. Chesi M, Nardini E, Brents LA, Schrock E, Ried T, Kuehl WM, et al. Frequent translocation t(4;14)(p16.3;q32.3) in multiple myeloma is associated with increased expression and activating mutations of fibroblast growth factor receptor 3. Nat Genet 1997;16(3):260–4. [PubMed: 9207791]
44. Richelda R, Ronchetti D, Baldini L, Cro L, Viggiano L, Marzella R, et al. A novel chromosomal translocation t(4; 14)(p16.3; q32) in multiple myeloma involves the fibroblast growth-factor receptor 3 gene. Blood 1997;90(10):4062–70. [PubMed: 9354676]
45. Dailey L, Laplantine E, Priore R, Basilico C. A network of transcriptional and signaling events is activated by FGF to induce chondrocyte growth arrest and differentiation. J Cell Biol 2003;161(6): 1053–66. [PubMed: 12821644]
46. Sarabipour S, Hristova K. Mechanism of FGF receptor dimerization and activation. Nat Commun 2016;7:10262. [PubMed: 26725515]
47. Kanai M, Goke M, Tsunekawa S, Podolsky DK. Signal transduction pathway of human fibroblast growth factor receptor 3. Identification of a novel 66-kDa phosphoprotein. J Biol Chem 1997;272(10):6621–8. [PubMed: 9045692]
48. Seo JH, Suenaga A, Hatakeyama M, Taiji M, Imamoto A. Structural and functional basis of a role for CRKL in a fibroblast growth factor 8-induced feed-forward loop. Molecular and cellular biology 2009;29(11):3076–87. [PubMed: 19307307]
49. Moon AM, Guris DL, Seo JH, Li L, Hammond J, Talbot A, et al. Crkl deficiency disrupts Fgf8 signaling in a mouse model of 22q11 deletion syndromes. Dev Cell 2006;10(1):71–80. [PubMed: 16399079]
50. Floyd SR, Pacold ME, Huang Q, Clarke SM, Lam FC, Cannell IG, et al. The bromodomain protein Brd4 insulates chromatin from DNA damage signalling. Nature 2013;498(7453):246–50. [PubMed: 23728299]

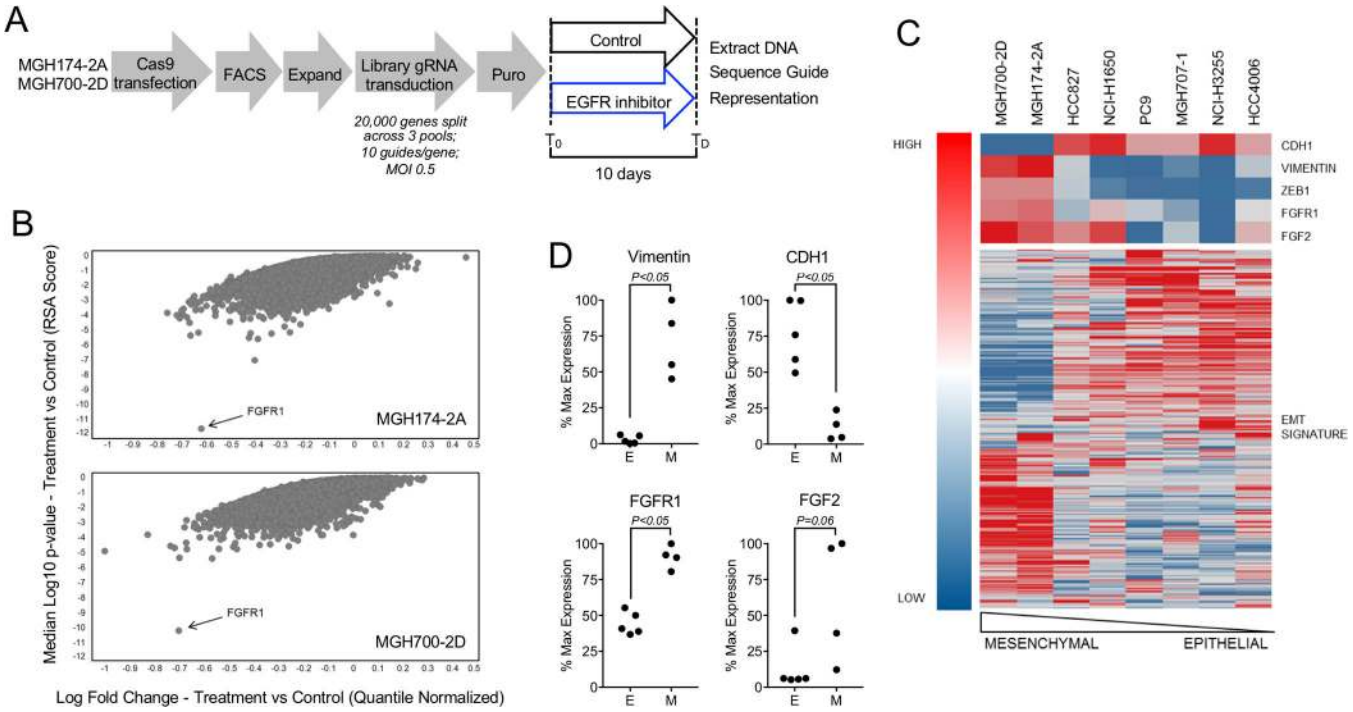

Figure 1. FGFR1 is a top genomic target for re-sensitizing patient-derived, mesenchymal cell lines to third generation EGFR TKI.

A, Experimental schema. B, Whole genome CRISPR/Cas9 screen with EGFR mutant mesenchymal-like cell lines MGH700–2D and MGH174–2A, with and without 100 nM EGF816. Modified volcano plot representing the aggregated guide performance for genes that sensitize (left) or activate (right) across mesenchymal-like cell lines to EGF816 based on median log fold change versus control. Y-axis is negative log10 p-values based on Stouffer's statistic. C, RNA-seq profiles of EGFR mutant NSCLC cell lines represent a spectrum of epithelial and mesenchymal-like phenotypes, as defined by an EMT signature profile (Loboda et al., 2011). Cell lines that returned FGFR1 as a hit in the CRISPR screen tended to be mesenchymal-like and/or had relatively higher expression of FGFR1 and FGF2. D, A broader collection of patient-derived epithelial (E) and mesenchymal-like (M) EGFR mutant NSCLC cell lines also demonstrate higher FGFR1 and FGF2 mRNA expression in the mesenchymal cell lines as determined by Affymetrix microarray. E – MGH119–1, MGH121–1, MGH34–1, MGH141–1, MGH157–1; M – MGH125, MGH126, MGH138–2A, MGH138–3F.

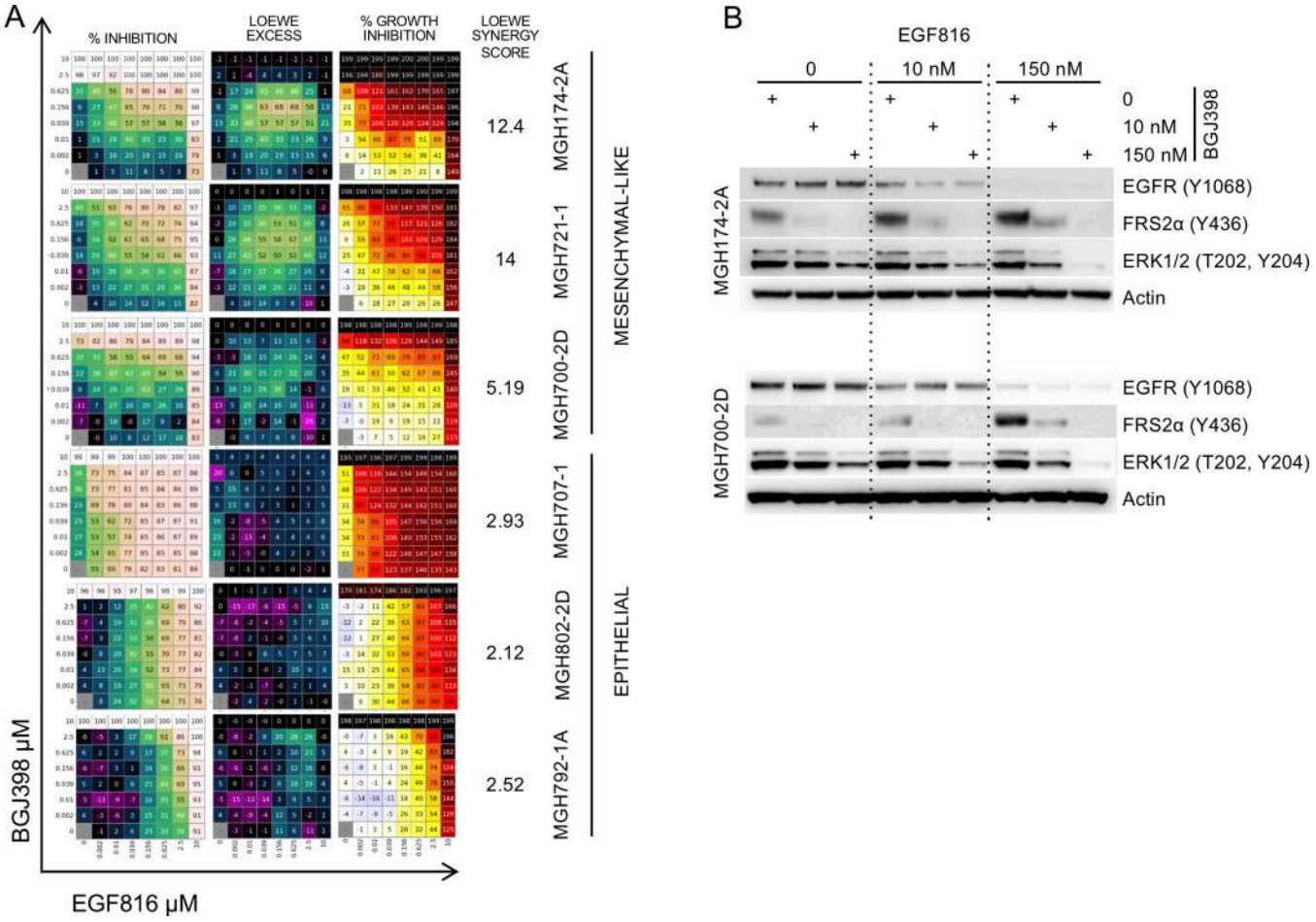

Figure 2. FGFR inhibition synergizes with EGFR TKI in mesenchymal, EGFR TKI-resistant cell lines.

A, EGFR-mutant patient derived cell lines were treated with an 8×8 combination matrix of EGF816 and BGJ398 titrations for 7 days. Synergy was observed in mesenchymal-like but not in epithelial cell lines. B, EGFR mutant mesenchymal-like patient derived cell lines treated with a 3×3 combination matrix of EGF816 and BGJ398 titrations for 24 hours. Combining EGFR and FGFR inhibitors leads to a reduction of downstream ERK1,2 phosphorylation.

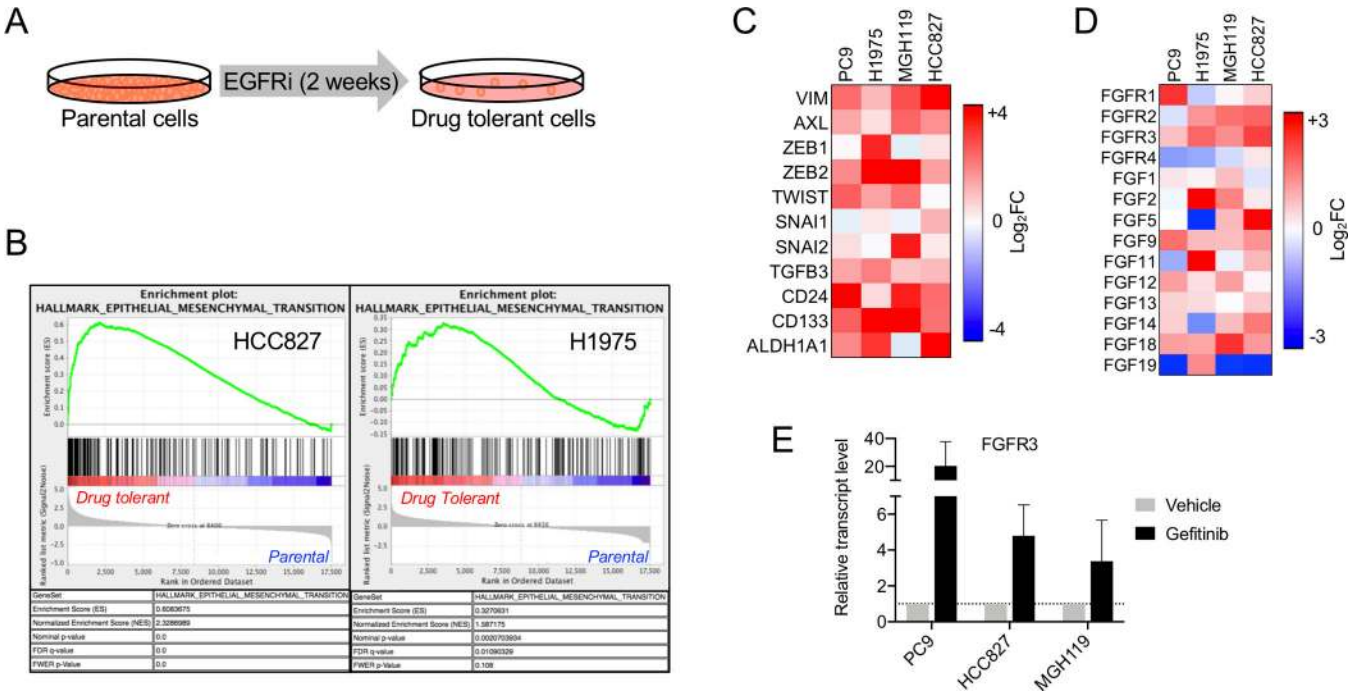

Figure 3. Increased expression of FGFR3 in EGFR TKI-sensitive cell lines undergoing EMT-like changes during drug treatment.

A, HCC827 and H1975 cells were treated for 2 weeks with 300 nM gefitinib or 1 μM WZ-4002, respectively. RNA-seq was performed to compare gene expression between untreated parental and surviving drug tolerant cells. B, GSEA revealed enrichment of genes related to EMT in drug tolerant cells relative to parental cells (mSigDB database, hallmarks gene sets). C, Genes related to EMT are increased after two weeks of EGFR TKI treatment are consistently upregulated in EGFR-mutated NSCLC lines. Relative gene expression (mean of 3 independent experiments) was determined by quantitative RT-PCR and is expressed as the log2 fold change in drug treated cells compared to untreated parental cells. D, Expression of FGF receptors and ligands in drug treated cells relative to untreated parental cells as determined by RNA-seq. E, FGFR3 is up-regulated after two weeks of EGFR TKI treatment as determined by quantitative RT-PCR. Data is shown as mean and SEM of two independent experiments.

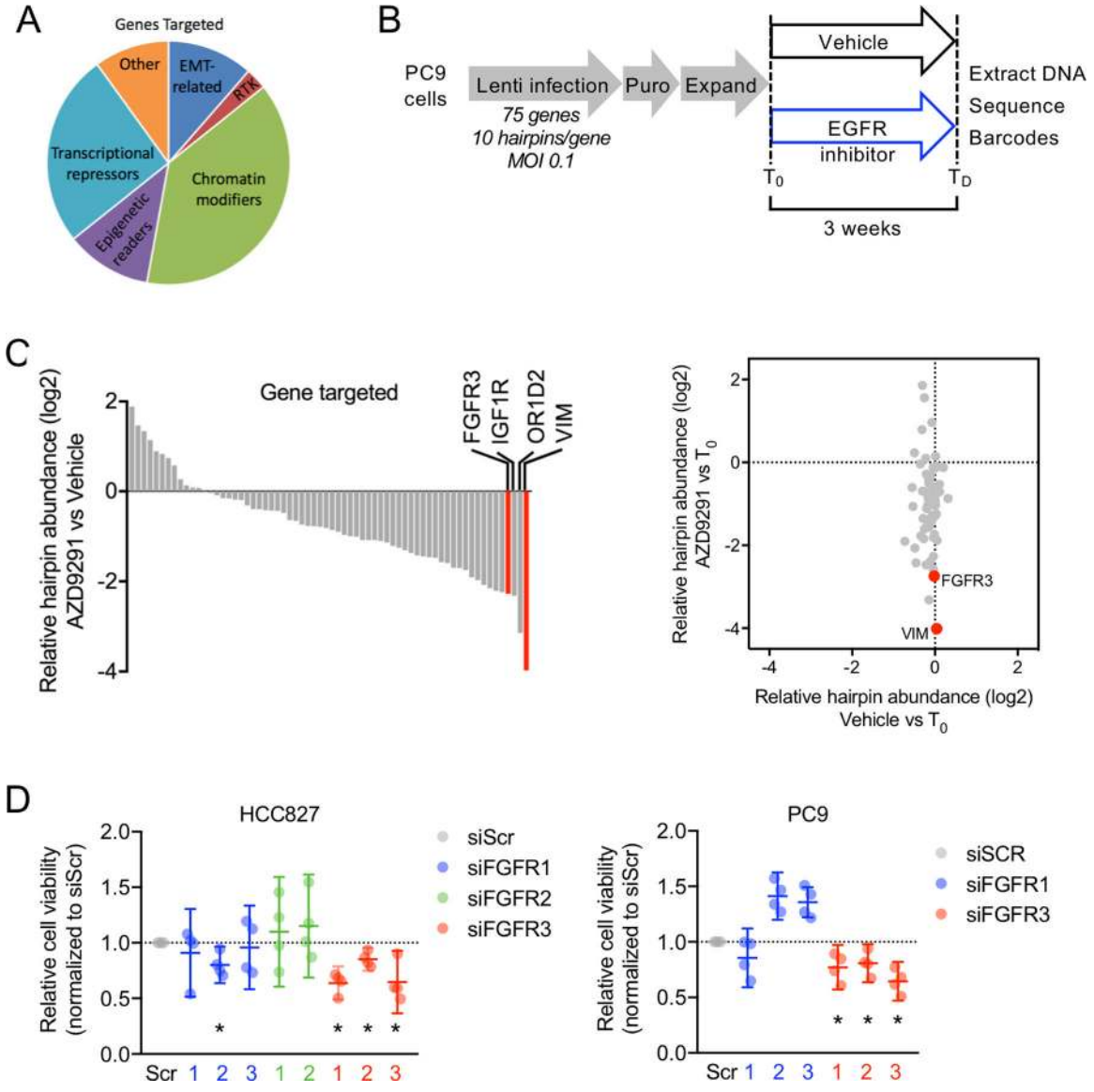

Figure 4. FGFR3 plays an essential role in the survival of EGFR mutant NSCLC drug tolerant cells.

A, Classification of genes targeted in the shRNA dropout mini-screen. B, Experimental schema. C, shRNA hairpins enriched/depleted after EGFR inhibitor treatment in PC9 cells. Left hand panel shows fold change in hairpin abundance of cells treated with osimertinib for 3 weeks compared to DMSO for 3 weeks. Right hand panel depicts change in hairpin abundance after 3 weeks of drug treatment versus 3 weeks of vehicle treatment. D, FGFR3 knockdown reduces survival of HCC827 and PC9 drug tolerant cells. Expression of FGFR receptors was suppressed by siRNA and cells were treated with were treated with gefitinib or vehicle for three days and cell viability determined. Values shown are the relative change in cell viability, normalized to scrambled siRNA control. Of note, FGFR2 expression was not reliably detected in PC9 cells. (Error bars are 95% confidence interval, four independent experiments; asterisks denote statistically significant $P<0.05$ decrease in cell viability with siFGFR relative to siScr, as described in Supplemental Figure 5).

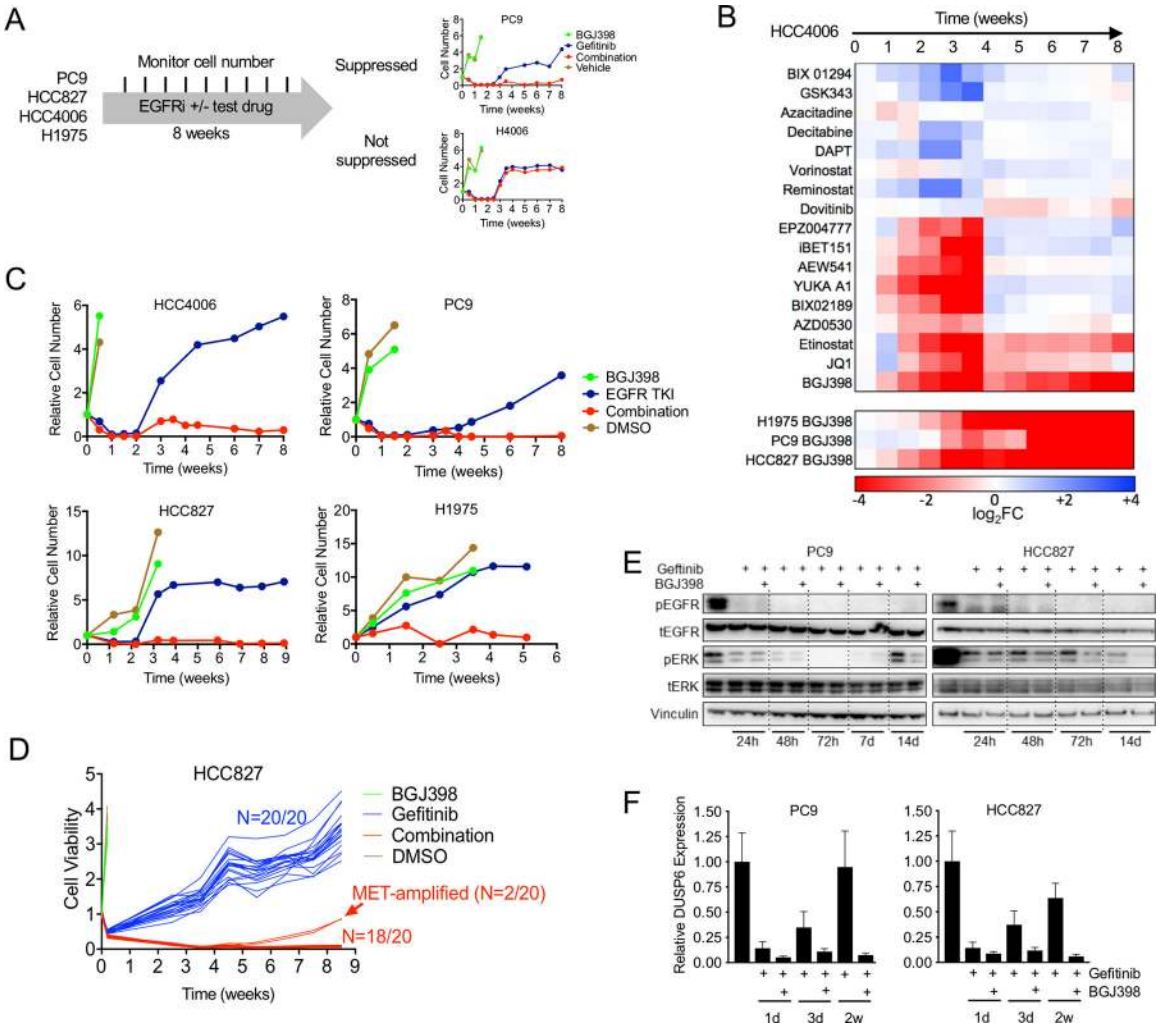

Figure 5. Dual EGFR-FGFR inhibition prevents the outgrowth of EGFR-mutant NSCLC drug tolerant clones.

A, Experimental schema. B, Relative decrease in cell number with gefitinib (300 nM) + test drug (100 nM) relative to gefitinib alone over time. Cell number was quantified by high content imaging. The bottom three rows show the response to gefitinib + BGJ398 for PC9 and HCC827 cells, WZ4002 + BGJ398 for H1975 cells. C, Individual growth curves of cell lines treated with gefitinib (300 nM) + BGJ398 (100 nM). D, RealTime-Glo assay of HCC827 cells were treated with gefitinib, BGJ398 or combination over time. E, PC9 and HCC827 cells were treated with gefitinib alone or in combination with BGJ398. The addition of BGJ398 to gefitinib prevented ERK reactivation. F, Addition of BGJ398 to gefitinib prevented DUSP6 upregulation, as assessed by RT-PCR. Data shown are mean and SEM of three independent experiments.

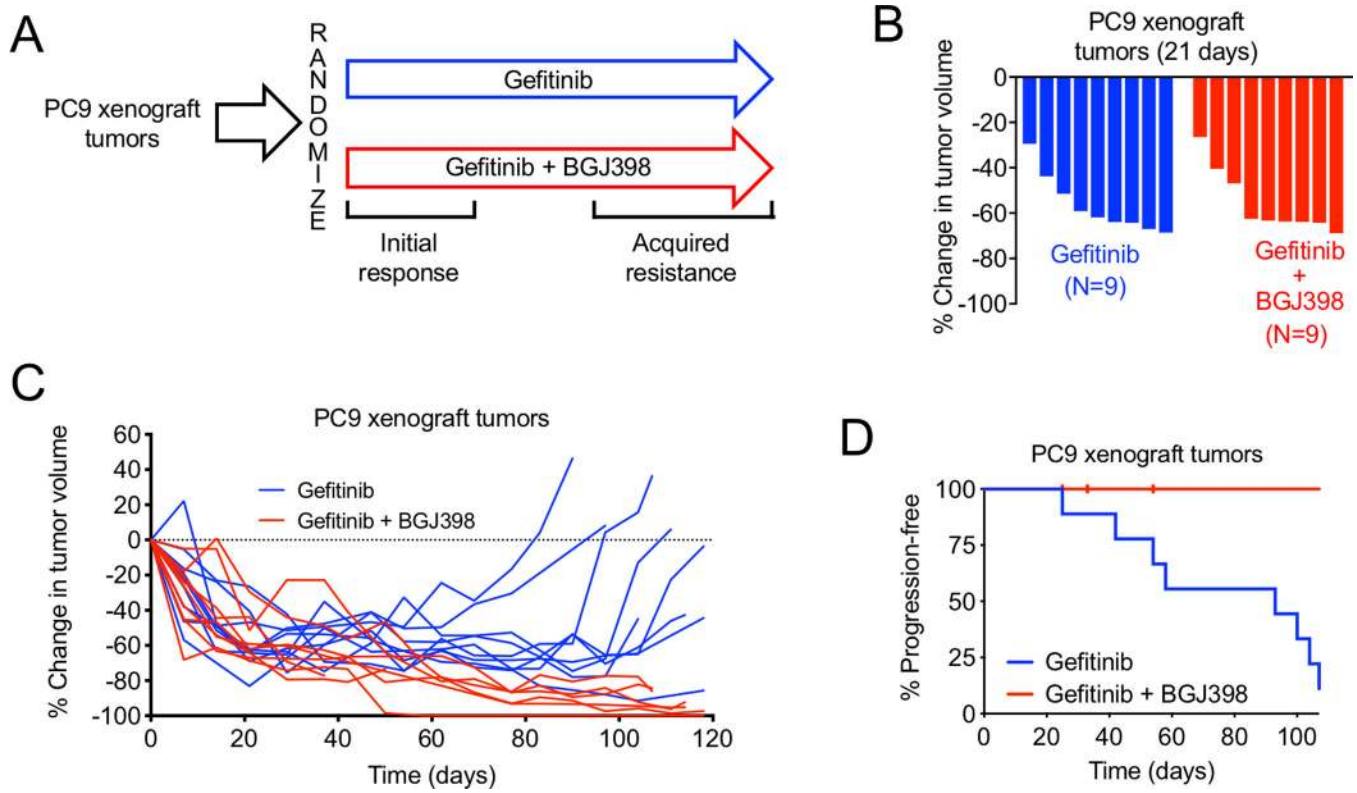

Figure 6. Combination EGFR + FGFR inhibition inhibits the development of resistance in vivo.

A, Experimental schema of PC9 xenograft efficacy study. B, Mice bearing PC9 xenograft tumors were treated with gefitinib (6.25 mg/kg daily) alone or in combination with BJG398 (30 mg/kg daily). Waterfall plot shows percent change in tumor volume after 21 days of drug treatment. C, After extended treatment, gefitinib but not combination treated tumors developed drug resistance. D, Kaplan-Meier curves showing time to 20% tumor regrowth (from minimum volume). Hashmarks indicate censored data from 3 combination treated mice that died during the course of the experiment from undetermined cause without evidence of tumor progression.